2 July 2026

Stability Trends of Surface and Subsurface Interstitial Transition Metal Species on CeO2(111)

Jelena Jelic, Yuemin Wang, Christof Wöll, Felix Studt

Abstract

Single-atom catalysts (SACs) on reducible oxides are generally assumed to consist of isolated metal atoms located at the surface and directly accessible to reactants. Recent studies on Pt/CeO_2(111), however, revealed that Pt preferentially occupies subsurface interstitial sites. Here, we investigate whether this behavior is unique to Pt or represents a more general phenomenon. Using density functional theory, we systematically compare the stability of surface and subsurface configurations for transition-metal atoms from Fe to Au on stoichiometric CeO_2(111). Pronounced periodic trends emerge: the tendency toward subsurface incorporation increases from the 3d to the 5d series and from the Fe group toward the Ni group, with Pt and Pd exhibiting the strongest preference. Several metals also induce oxygen migration and surface reconstruction, generating additional stable configurations. Calculated CO vibrational frequencies provide spectroscopic fingerprints for experimental identification. These results demonstrate that subsurface incorporation is a general structural motif in SACs on reducible oxides, challenging the conventional view of surface-bound single-atom catalysts.

Keywords

Cerium dioxide, Density functional theory, Interstitial sites, IR spectroscopy, Single-atom catalysts, Transition metals

Stability Trends of Surface and Subsurface Interstitial Transition Metal Species on $CeO_2(111)$

Jelena Jelic,[a] Yuemin Wang,[b,*] Christof Wöll,[b,c,*] and Felix Studt [a,d,*]

[a] Institute of Catalysis Research and Technology (IKFT), Karlsruhe Institute of Technology (KIT), 76344 Eggenstein-Leopoldshafen, Germany

[b] Institute of Functional Interfaces (IFG), Karlsruhe Institute of Technology (KIT), 76344 Eggenstein-Leopoldshafen, Germany

[c] Ordos Laboratory, Ordos, Inner Mongolia, China

[d] Institute for Chemical Technology and Polymer Chemistry (ICTP), Karlsruhe Institute of Technology (KIT), 76131 Karlsruhe, Germany

*Corresponding authors: yuemin.wang@kit.edu; christof.woell@kit.edu; felix.studt@kit.edu

ABSTRACT: Single-atom catalysts (SACs) on reducible oxides are generally assumed to consist of isolated metal atoms located at the surface and directly accessible to reactants. Recent studies on Pt/CeO_2(111), however, revealed that Pt preferentially occupies subsurface interstitial sites. Here, we investigate whether this behavior is unique to Pt or represents a more general phenomenon. Using density functional theory, we systematically compare the stability of surface and subsurface configurations for transition-metal atoms from Fe to Au on stoichiometric CeO_2(111). Pronounced periodic trends emerge: the tendency toward subsurface incorporation increases from the 3d to the 5d series and from the Fe group toward the Ni group, with Pt and Pd exhibiting the strongest preference. Several metals also induce oxygen migration and surface reconstruction, generating additional stable configurations. Calculated CO vibrational frequencies provide spectroscopic fingerprints for experimental identification. These results demonstrate that subsurface incorporation is a general structural motif in SACs on reducible oxides, challenging the conventional view of surface-bound single-atom catalysts.

Keywords: Cerium dioxide • Density functional theory • Interstitial sites • IR spectroscopy • Single-atom catalysts • Transition metals

TOC GRAPHIC

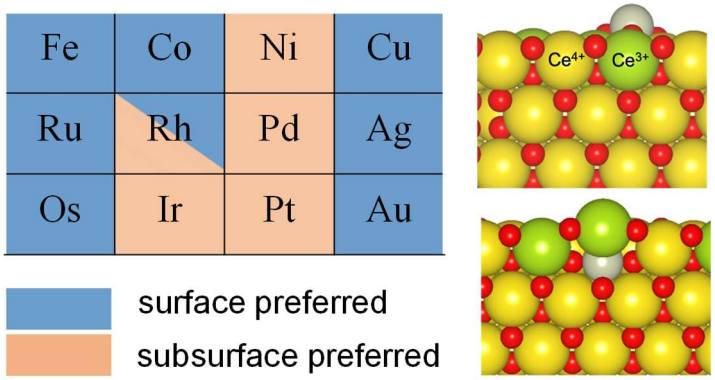

1. Introduction

Single-atom catalysis (SAC) has emerged as a central concept in heterogeneous catalysis, combining maximal atom efficiency with catalytic properties that are fundamentally distinct from those of nanoparticles and extended metal surfaces.[1-8] By stabilizing isolated metal atoms on suitable supports, SAC systems often exhibit exceptional activity, selectivity, and stability while minimizing the consumption of scarce noble metals such as Pt, Pd, Rh, or Ir. [9]

Since the pioneering demonstration of CO oxidation on Pt_1/FeO_x catalysts,[1] tremendous efforts have been devoted to identifying support materials capable of stabilizing isolated metal atoms under realistic reaction conditions. Among the most important classes of supports are reducible oxides, in particular cerium dioxide (CeO_2), whose oxygen-storage capability and facile Ce^{4+}/Ce^{3+} redox chemistry strongly influences the electronic structure and catalytic properties of supported metal species. [2, 10-13]

For Pt/CeO_2 systems, isolated Pt atoms have been widely invoked as active sites in reactions such as CO oxidation, the water–gas shift reaction, and selective hydrogenation.[9, 14-17] In most theoretical and experimental studies, these single atoms are assumed to occupy adsorption sites at the oxide surface, where they remain directly accessible to reactants. However, despite extensive investigations, the actual geometric and electronic structures of isolated metal species on ceria remains controversial.[10, 16-23] In particular, the dynamic nature of metal–ceria interactions, together with the redox flexibility of the support, complicates the identification of stable atomic configurations under realistic conditions. This situation strongly contrasts with that of homogeneous catalysis, where transition metal atoms with well-defined ligands are utilized. Metal–organic frameworks (MOFs) represent the heterogenous counterpart, providing similarly well-defined coordination environments that enable isolated, homogeneously dispersed metal sites to be structurally characterized with high precision. [24, 25] For isolated metal atoms deposited on oxide surfaces, however, the geometric structure and local coordination environment are frequently much less well defined, making their knowledge-based optimization inherently difficult.

Recently, we reported combined experimental and theoretical evidence revealing that Pt atoms deposited on $CeO_2(111)$ do not predominantly remain as surface adatoms at low coverages; instead, they preferentially occupy subsurface interstitial positions beneath the outermost oxide layer, a configuration not previously recognized.[26] Using polarization-resolved infrared reflection–absorption spectroscopy (IRRAS), grazing-emission X-ray photoelectron

spectroscopy (XPS), and density functional theory (DFT) calculations, we demonstrated that the experimentally observed blue-shifted CO vibrational band at ~2169 cm^{-1} is inconsistent with conventional surface-bound Pt single atoms. Instead, the data are fully consistent with Pt atoms incorporated into interstitial sites below the $CeO_2(111)$ surface. These subsurface configurations are thermodynamically favored relative to surface-bound Pt adatoms and remain inaccessible to direct CO adsorption. The results challenge the prevailing assumption that isolated metal atoms in SAC systems necessarily reside at the surface.[26]

The identification of subsurface interstitial Pt single atoms immediately raises a broader and highly relevant question: Is such subsurface stabilization unique to platinum, or does it represent a more general phenomenon for metal atoms on reducible oxide surfaces? Addressing this issue is essential for understanding the structural motifs that govern SAC stability and catalytic functionality on ceria. In particular, the balance among lattice strain, oxidation-state stabilization, metal–oxygen coordination, and redox compensation may depend strongly on the nature of the deposited metal atom. Systematic theoretical investigations across different transition metals are therefore required to establish trends governing the competition between surface adsorption and subsurface incorporation. In addition to determining the location of metal atoms on oxide surfaces using electronic structure calculations, it is essential to identify experimental observables that allow their unambiguous characterization. Among the available approaches, surface-ligand infrared spectroscopy (SLIR) has emerged as a particularly powerful tool for this purpose.[27, 28] By bridging the materials and pressure gaps between model surfaces and powder catalysts,[29, 30] and in combination with accurate frequency calculations, [31, 32] CO-SLIR offers a unique framework for identifying isolated metal species on oxide surfaces and for distinguishing different coordination environments in metal clusters and nanoparticles. [33-37]

In the present work, we carry out a systematic DFT investigation of eleven additional transition-metal atoms ranging from Fe to Au on stoichiometric $CeO_2(111)$, with a particular focus on the competition between conventional surface adsorption sites and subsurface interstitial configurations. In addition, we calculate the vibrational frequencies of adsorbed CO as an experimental observable for identifying these species by infrared spectroscopy.

2. Computational Methods

Density functional theory (DFT) calculations have been performed using the Vienna Ab Initio Simulation Package (VASP) in version 5.4.3 [38, 39] using analogous parameters as in previous work.[26] Briefly, all calculations were spin polarized and employed the Bayesian Error Estimation Functional with van der Waals correlation (BEEF-vdW)[40] using the projector-augmented wave method (PAW) with standard PAW potentials.[41] A plane wave basis set with an energy cutoff of 450 eV and a Gaussian smearing with a width of 0.1 eV have been used. In order to describe the delocalized Ce f orbitals more accurately, we applied the GGA+U method,[42] with U being 5.0 eV as obtained from earlier work.[43] Convergence of the SCF cycle was set at an energy difference of 10^{-7} eV, while ionic convergence was achieved when all atomic forces were below 0.01 eV/Å. As the calculated vibration of CO is slightly off the experimental value, we used a scaling factor of 1.0086 for all CO vibrations.

All calculations used periodic 3x3x3 large ceria slabs with the CeO_2(111) surface termination, that were separated by more than 15 Å of vacuum in the z-direction. The bottom row of atoms was kept in their bulk positions, while the two uppermost layers and all other atoms were allowed to relax during geometry optimization. The Brillouin zone was sampled using a 2x2x1 Monkhorst-Pack k-point grid.[44] The single-atom configurations considered in the work are (1) a transition metal on the surface of CeO_2(111), (2) a transition metal on the surface of CeO_2(111) with an oxygen having migrated from the CeO_2 lattice ontop of the transition metal, (3) a transition metal being located in the subsurface of CeO_2(111) and (4) a transition metal in the subsurface of CeO_2(111) where a CeO_2 unit has been removed from the top layer. We investigated all the 11 late transition metals next to Pt, namely Fe, Ru, Os, Co, Rh, Ir, Ni, Pd, Cu, Ag and Au. CO adsorption and vibrations have been considered on all surfaces. Vibrational analyses were performed using the harmonic approximation with the finite difference method employing displacements of 0.01 Å.

3. Results and Discussion

Figure 1 presents four DFT-optimized surface and subsurface adsorption configurations of Rh single atoms on $CeO_2(111)$, which serve as representative examples of the adsorption geometries considered for the 12 transition metals (Fe–Au) examined in this work. All investigated metals are initially treated in their neutral M^0 state, analogous to the $Pt/CeO_2(111)$ system investigated previously.[26] The calculated binding energies of the 12 single-atom metals in the different adsorption geometries are summarized in Table 1.

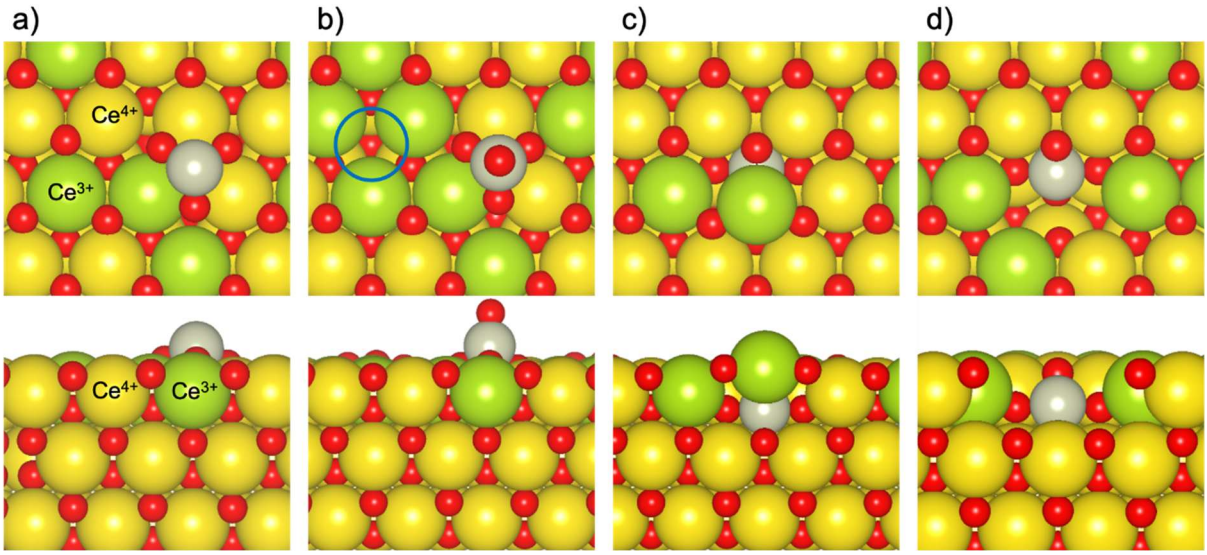

Figure 1. Top and side view of the four different configurations of the transition metals considered in this study, shown for the case of Rh single atoms at the $CeO_2(111)$ surface. Configurations are a) Rh on the surface of $CeO_2(111)$ (denoted $M/CeO_2(111)$; b) Rh on the surface of $CeO_2(111)$ with an oxygen from the CeO_2 (blue circle) migrated ontop of the metal (denoted $MO/CeO_2(111)_v$; c) Rh occupying interstitial subsurface sites of $CeO_2(111)$ (denoted $M_{sub}/CeO_2(111)$ and d) Rh in the subsurface of $CeO_2(111)$ where a CeO_2 unit has been removed from the top layer (denoted $M_{sub}/CeO_2(111)_{CeO2vac}$. Color code: orange – Ce^{4+}, green – Ce^{3+}, red – O, gray – Rh.

Pronounced periodic trends emerge from the calculations. When considering only the relative stability of surface and subsurface interstitial geometries, the tendency toward subsurface interstitial incorporation increases systematically from the 3d to the 5d transition-metal series and from the Fe group toward the Ni group. Subsurface interstitial configurations are stabilized for Ir, Ni, Pd and Pt single atoms, whereas Fe, Ru, Os, Co, and the coinage metals Cu, Ag, and Au favor surface adsorption (see Figure 2a). Figure 2b shows the periodic-table trend in the

stability of surface- and subsurface-bound transition-metal single atoms. At the BEEF-vdW level of theory, Pt exhibits the strongest preference for subsurface incorporation (−0.54 eV relative to the surface configuration), followed by Pd (−0.29 eV), whereas Ag strongly disfavors subsurface occupation (+2.21 eV).

Table 1. Calculated binding energies (eV) of 12 transition-metal single atoms in various surface and subsurface configurations illustrated in Figure 1, referenced to the $CeO_2(111)$ slab, the corresponding bulk metal, and the CeO_2 bulk.

transition metal	surface		subsurface	
	$M/CeO_2(111)$ ΔE_M (eV)	$MO/CeO_2(111)_v$ ΔE_M (eV)	$M_{sub}/CeO_2(111)$ ΔE_M (eV)	$M_{sub}/CeO_2(111)_{CeO2vac}$ ΔE_M (eV)
Fe	-1.00	-0.35	-0.42	-1.17
Ru	0.40	-0.01	1.05	0.39
Os	0.74	-0.41	1.54	0.61
Co	-0.18	0.77	0.40	-0.08
Rh	1.25	1.45	1.29	1.07
Ir	1.92	1.51	1.81	1.34
Ni	0.18	1.84	0.11	0.47
Pd	1.45	2.70	1.16	1.09
Pt	1.76	3.28	1.22	1.33
Cu	0.50	2.31	1.18	0.74
Ag	0.47	2.96	2.69	2.10
Au	1.40	2.48	2.28	1.80

The calculations further reveal that the structural landscape is considerably more complex than a simple surface-versus-subsurface picture. For several metals, the migration of oxygen atoms from the ceria lattice toward surface-bound metal atoms is energetically favorable, forming strongly stabilized M–O species accompanied by oxygen vacancies in the oxide lattice (see Figure 1b, Table 1). This behavior is particularly pronounced for Ir, where an $IrO/CeO_2(111)_v$ configuration is calculated to be more stable than the corresponding subsurface geometry. In addition, for selected metals such as Pd, Rh, Ir, and Fe, removal of a surface CeO_2 unit gives rise to highly stable reconstructed structures involving subsurface metal incorporation. These findings demonstrate that isolated metal atoms on reducible oxides may adopt a rich variety of structural motifs governed by a delicate interplay among redox chemistry, lattice relaxation, and metal–oxygen bond formation.

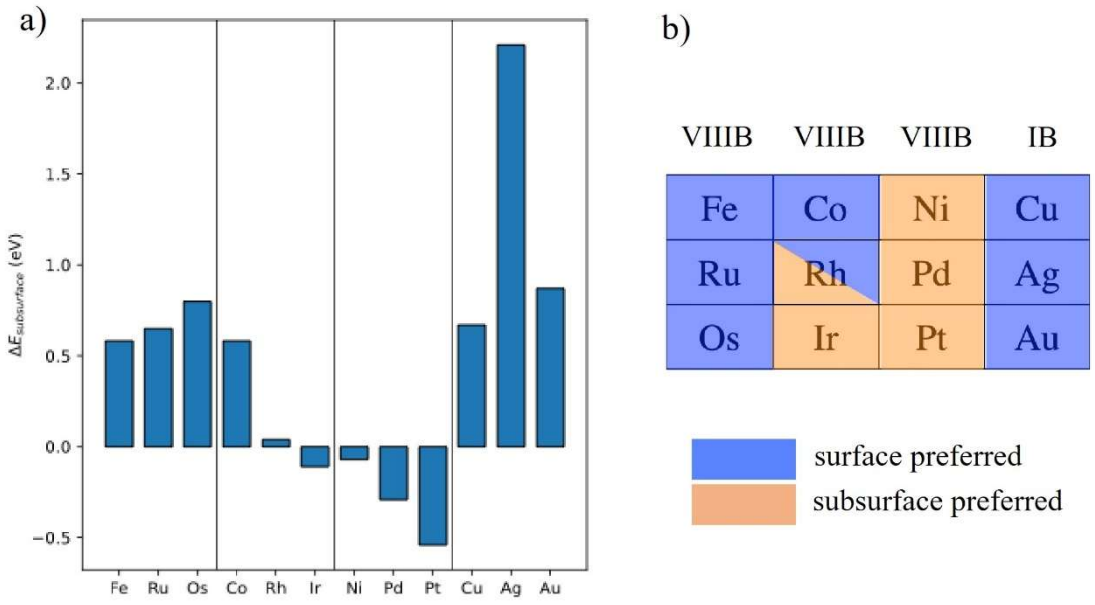

Figure 2. a) Calculated relative energies (ΔE, eV) for 12 transition-metal single atoms at subsurface interstitial sites in $CeO_2(111)$ ($M_{sub}/CeO_2(111)$, configuration c in Figure 1), relative to surface-bound states ($M/CeO_2(111)$, configuration a in Figure 1); b) stability trends of surface- and subsurface-bound transition-metal single atoms mapped onto the periodic table.

Our earlier work suggested that CO can be used as a probe molecule to investigate whether a transition metal occupies a subsurface interstitial site, where the CO stretching frequency is blue-shifted relative to the gas-phase CO value, reaching ~2169 cm^{-1} in the case of $Pt/CeO_2(111)$.[26] In contrast, CO adsorbed atop a transition metal on the $CeO_2(111)$ surface exhibits a significantly redshifted vibrational frequency.[26] We therefore calculated CO adsorption on both surface and subsurface interstitial transition metal sites, an example for $Rh/CeO_2(111)$ is displayed in Figure 3.

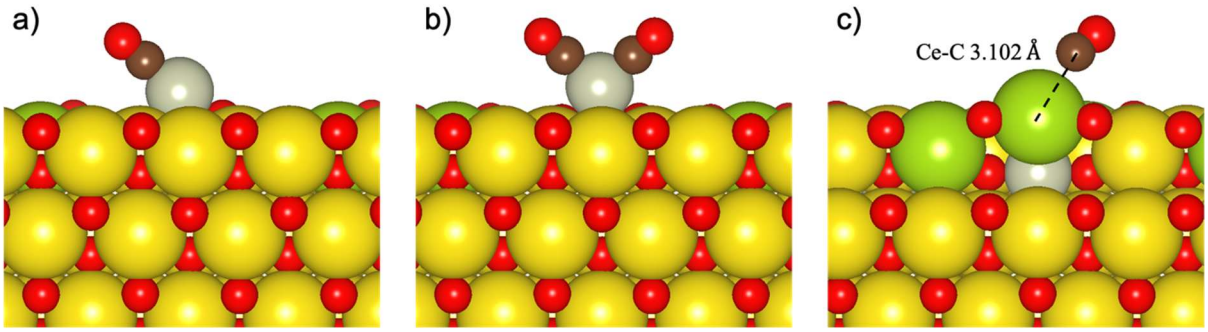

Figure 3. DFT-optimized structures of CO binding to distinct single-atom Rh/CeO_2(111) model catalysts: a) CO–Rh on Rh/CeO_2(111), b) 2xCO–Rh on Rh/CeO_2(111) and c) CO–Ce^{3+} on Rh_{sub}/CeO_2(111) where interstitial Pt is stabilized in the subsurface of CeO_2(111). Color code: orange – Ce^{4+}, green– Ce^{3+}, red – O, gray – Rh, brown – C.

As expected, our calculations of CO binding strengths and vibrational frequencies show that the strongest adsorption occurs when transition-metal single atoms adopt the surface configuration (M/CeO_2(111), Figure 1a). In this case, adsorption energies range from -0.7 to -2.35 eV (Table 2), with Pt and Au exhibiting the strongest CO binding. In fact, the binding is often so strong that a second CO can bind to the metal center, as evidenced by two distinct CO stretching vibrations observed experimentally.[45,46] By contrast, CO adsorption on M_{sub}/CeO_2(111) (configuration c in Figure 1), where transition-metal single atoms are stabilized at subsurface interstitial sites, is considerably weaker, with adsorption energies of -0.2 to -0.3 eV, corresponding to physisorbed CO dominated by dispersion interactions. Likewise, CO adsorbed on surface transition-metal sites exhibits red-shifted vibrational frequencies, and we also calculated the characteristic two-band signatures for adsorption of two CO molecules (Table 2). In pronounced contrast, CO vibrations associated with subsurface transition metals are blue-shifted relative to the gas-phase CO frequency, falling within a narrow range of 2165–2176 cm^{-1} (Table 2). This distinctive spectral feature suggests that CO can serve as a sensitive probe for identifying subsurface transition-metal configurations. For a systematic comparison, Tables S1–S4 summarize the calculated adsorption energies and corresponding vibrational frequencies of various CO species adsorbed on surface Ce^{4+} and Ce^{3+} sites across the four single atom configurations considered for 12 transition metals on CeO_2(111) (see Figure 1).

Table 2. Calculated CO adsorption energies and corresponding vibrational frequencies for the surface and subsurface configuration of the 12 transition metals at the $CeO_2(111)$ surface. CO vibrational frequencies are scaled using a factor of 1.008.

transition metal	surface			subsurface	
	ΔE_{CO} (eV)[2]	CO υ_{CO} (cm^{-1})	2xCO υ_{CO} (cm^{-1})	ΔE_{CO} (eV)	CO υ_{CO} (cm^{-1})
Fe	-0.78 / 0.03	2112	2016/1972	-0.27	2165
Ru	-1.41 / -0.06	2019	2034/1979	-0.28	2167
Os	-1.78 / -0.80	1995	2029/1970	-0.32	2169
Co	-0.70 / -0.84	2089	2047/2004	-0.28	2170
Rh	-1.39 / -1.98	1990	2068/2009	-0.30	2165
Ir	-2.03/-1.94	2025	2025/2004	-0.58	2176
Ni	-0.76 / -0.55	2082	2069/2033	-0.30	2167
Pd	-1.81 / -0.84	2034	2129/2093	-0.31	2168
Pt[1]	-2.22 / -1.33	2031	2118/2067	-0.29	2174
Cu	-1.58 / -0.19	2029	2138/2101	-0.30	2168
Ag	-0.89 / 0.26	2142	2145/2132	-0.30	2170
Au	-2.31/ 0.66	2116	2121/2098	-0.30	2170

[1] taken from ref. [26], [2] differential binding energy of the first and second CO molecule.

4. Conclusions

In summary, our systematic DFT calculations on 12 transition-metals spanning Fe to Au reveal periodic trends in the thermodynamic stability of transition-metal single atoms on $CeO_2(111)$, with subsurface interstitial species becoming progressively more favorable relative to surface species from the 3d to the 5d series and from the Fe to the Ni group. Oxygen migration and surface reconstruction further diversify the accessible energy landscape, giving rise to multiple low-energy configurations and a structural complexity beyond the conventional picture of single-atom catalysts. The calculated CO vibrational frequencies provide distinct spectroscopic fingerprints that enable experimental discrimination between surface- and subsurface-bound species. Collectively, these findings demonstrate that subsurface interstitial incorporation is not an isolated peculiarity of Pt but rather a general structural motif for transition-metal single atoms on reducible oxide supports. Our results challenge the prevailing surface-bound assumption for single-atom catalysts, with important implications for their characterization, mechanistic interpretation, and rational design.

ASSOCIATED CONTENT

Supporting Information

Additional DFT data (Tables S1-S4), coordinates of all DFT-optimized structures (PDF)

Notes

The authors declare no competing financial interests.

ACKNOWLEDGMENTS

This work was funded by the Deutsche Forschungsgemeinschaft (DFG, German Research Foundation) – Project-ID 426888090 – SFB 1441. The authors acknowledge support by the state of Baden-Württemberg through bwHPC and the German Research Foundation (DFG) through grant no. INST40/575-1FUGG (JUSTUS2 cluster, RVs bw17D011). Support from the Helmholtz Association is also gratefully acknowledged.

REFERENCES

1. Qiao, B.; Wang, A.; Yang, X.; Allard, L. F.; Jiang, Z.; Cui, Y.; Liu, J.; Li, J.; Zhang, T., Single-atom catalysis of CO oxidation using Pt1/FeO x. *Nat. Chem.* **2011,** *3* (8), 634-641.
2. Fu, Q.; Saltsburg, H.; Flytzani-Stephanopoulos, M., Active nonmetallic Au and Pt species on ceria-based water-gas shift catalysts. *Science* **2003,** *301* (5635), 935-938.
3. Muravev, V.; Spezzati, G.; Su, Y.-Q.; Parastaev, A.; Chiang, F.-K.; Longo, A.; Escudero, C.; Kosinov, N.; Hensen, E. J., Interface dynamics of Pd–CeO_2 single-atom catalysts during CO oxidation. *Nat. Catal.* **2021,** *4* (6), 469-478.
4. Cui, X.; Li, W.; Ryabchuk, P.; Junge, K.; Beller, M., Bridging homogeneous and heterogeneous catalysis by heterogeneous single-metal-site catalysts. *Nat. Catal.* **2018,** *1* (6), 385-397.
5. Hulva, J.; Meier, M.; Bliem, R.; Jakub, Z.; Kraushofer, F.; Schmid, M.; Diebold, U.; Franchini, C.; Parkinson, G. S., Unraveling CO adsorption on model single-atom catalysts. *Science* **2021,** *371* (6527), 375-379.
6. Kaiser, S. K.; Chen, Z. P.; Akl, D. F.; Mitchell, S.; Pérez-Ramírez, J., Single-Atom Catalysts across the Periodic Table. *Chemical Reviews* **2020,** *120* (21), 11703-11809.
7. Shi, X.; Wen, Z.; Gu, Q.; Jiao, L.; Jiang, H.-L.; Lv, H.; Wang, H.; Ding, J.; Lyons, M. P.; Chang, A., Metal–support frontier orbital interactions in single-atom catalysis. *Nature* **2025**, 1-8.
8. Liu, L.; Corma, A., Metal catalysts for heterogeneous catalysis: from single atoms to nanoclusters and nanoparticles. *Chem. Rev.* **2018,** *118* (10), 4981-5079.
9. Wang, A.; Li, J.; Zhang, T., Heterogeneous single-atom catalysis. *Nat. Rev. Chem.* **2018,** *2* (6), 65-81.
10. Li, X.; Pereira-Hernández, X. I.; Chen, Y.; Xu, J.; Zhao, J.; Pao, C.-W.; Fang, C.-Y.; Zeng, J.; Wang, Y.; Gates, B. C., Functional CeO x nanoglues for robust atomically dispersed catalysts. *Nature* **2022,** *611* (7935), 284-288.
11. Jones, J.; Xiong, H.; DeLaRiva, A. T.; Peterson, E. J.; Pham, H.; Challa, S. R.; Qi, G.; Oh, S.; Wiebenga, M. H.; Pereira Hernández, X. I., Thermally stable single-atom platinum-on-ceria catalysts via atom trapping. *Science* **2016,** *353* (6295), 150-154.
12. Trovarelli, A.; Llorca, J., Ceria Catalysts at Nanoscale: How Do Crystal Shapes Shape Catalysis? *ACS Catalysis* **2017,** *7* (7), 4716-4735.
13. Daelman, N.; Capdevila-Cortada, M.; López, N., Dynamic charge and oxidation state of Pt/CeO_2 single-atom catalysts. *Nat. Mater.* **2019,** *18* (11), 1215-1221.
14. Gänzler, A. M.; Casapu, M.; Vernoux, P.; Loridant, S.; Cadete Santos Aires, F. J.; Epicier, T.; Betz, B.; Hoyer, R.; Grunwaldt, J. D., Tuning the structure of platinum particles on ceria in situ for enhancing the catalytic performance of exhaust gas catalysts. *Angew Chem Int Ed* **2017,** *56* (42), 13078-13082.
15. Ding, K.; Gulec, A.; Johnson, A. M.; Schweitzer, N. M.; Stucky, G. D.; Marks, L. D.; Stair, P. C., Identification of active sites in CO oxidation and water-gas shift over supported Pt catalysts. *Science* **2015,** *350* (6257), 189-192.
16. Nie, L.; Mei, D.; Xiong, H.; Peng, B.; Ren, Z.; Hernandez, X. I. P.; DeLaRiva, A.; Wang, M.; Engelhard, M. H.; Kovarik, L., Activation of surface lattice oxygen in single-atom Pt/CeO_2 for low-temperature CO oxidation. *Science* **2017,** *358* (6369), 1419-1423.
17. Zhang, Z.; Tian, J.; Lu, Y.; Yang, S.; Jiang, D.; Huang, W.; Li, Y.; Hong, J.; Hoffman, A. S.; Bare, S. R., Memory-dictated dynamics of single-atom Pt on CeO_2 for CO oxidation. *Nat. Commun.* **2023,** *14* (1), 2664.
18. Jeong, H.; Kwon, O.; Kim, B.-S.; Bae, J.; Shin, S.; Kim, H.-E.; Kim, J.; Lee, H., Highly durable metal ensemble catalysts with full dispersion for automotive applications beyond single-atom catalysts. *Nat. Catal.* **2020,** *3* (4), 368-375.
19. Wang, H.; Liu, J.-X.; Allard, L. F.; Lee, S.; Liu, J.; Li, H.; Wang, J.; Wang, J.; Oh, S. H.; Li, W., Surpassing the single-atom catalytic activity limit through paired Pt-O-Pt ensemble built from isolated Pt1 atoms. *Nat. Commun.* **2019,** *10* (1), 3808.

20. Sarma, B. B.; Maurer, F.; Doronkin, D. E.; Grunwaldt, J.-D., Design of single-atom catalysts and tracking their fate using operando and advanced X-ray spectroscopic tools. *Chem. Rev.* **2022,** *123* (1), 379-444.
21. Jiang, D.; Yao, Y.; Li, T.; Wan, G.; Pereira-Hernández, X. I.; Lu, Y.; Tian, J.; Khivantsev, K.; Engelhard, M. H.; Sun, C., Tailoring the local environment of platinum in single-atom Pt_1/CeO_2 catalysts for robust low-temperature CO oxidation. *Angew Chem Int Ed* **2021,** *133* (50), 26258-26266.
22. Maurer, F.; Jelic, J.; Wang, J.; Gänzler, A.; Dolcet, P.; Wöll, C.; Wang, Y.; Studt, F.; Casapu, M.; Grunwaldt, J.-D., Tracking the formation, fate and consequence for catalytic activity of Pt single sites on CeO_2. *Nat. Catal.* **2020,** *3* (10), 824-833.
23. Bohigues, B.; Rojas-Buzo, S.; Salusso, D.; Xia, Y.; Corma, A.; Bordiga, S.; Boronat, M.; Willhammar, T.; Moliner, M.; Serna, P., Overcoming activity/stability tradeoffs in CO oxidation catalysis by Pt/CeO2. *Nature Communications* **2025,** *16* (1), 7451.
24. Rogge, S. M. J.; Bavykina, A.; Hajek, J.; Garcia, H.; Olivos-Suarez, A. I.; Sepúlveda-Escribano, A.; Vimont, A.; Clet, G.; Bazin, P.; Kapteijn, F.; Daturi, M.; Ramos-Fernandez, E. V.; Xamena, F.; Van Speybroeck, V.; Gascon, J., Metal-organic and covalent organic frameworks as single-site catalysts. *Chemical Society Reviews* **2017,** *46* (11), 3134-3184.
25. Wang, W.; Sharapa, D. I.; Chandresh, A.; Nefedov, A.; Heißler, S.; Heinke, L.; Studt, F.; Wang, Y.; Wöll, C., Interplay of Electronic and Steric Effects to Yield Low-Temperature CO Oxidation at Metal Single Sites in Defect-Engineered HKUST-1. *Angew Chem Int Ed* **2020,** *59* (26), 10514-10518.
26. Chen, S.; Yu, Z.; Wang, J.; Jelic, J.; Li, W.; Studt, F.; Wang, Y.; Wöll, C., Subsurface Stabilization of Interstitial Pt Atoms on CeO₂ (111): Rethinking Single-Atom Catalyst Architectures. *Angew Chem Int Ed* **2026,** *65*, e22372.
27. Wöll, C., Structure and chemical properties of oxide nanoparticles determined by surface-ligand IR spectroscopy. *ACS Catal.* **2019,** *10* (1), 168-176.
28. Yang, C.; Idriss, H.; Wang, Y.; Wöll, C., Surface structure and chemistry of CeO_2 powder catalysts determined by surface-ligand infrared spectroscopy (SLIR). *Acc. Chem. Res.* **2024,** *57* (22), 3316-3326.
29. Caulfield, L.; Sauter, E.; Idriss, H.; Wang, Y. M.; Wöll, C., Bridging the Pressure and Materials Gap in Heterogeneous Catalysis: A Combined UHV, In Situ, and Operando Study Using Infrared Spectroscopy. *J. Phys. Chem. C* **2023,** *127* (29), 14023-14029.
30. Caulfield, L.; Yu, Z. R.; Gu, Y.; Yang, C. W.; Falkner, S.; Weidler, P.; Schwotzer, M.; Feldmann, C.; Wang, Y. M.; Wöll, C., Tracking Facet-Dependent Surface Transformations of Ceria Nanoparticles from UHV to Ambient Pressure via Infrared Spectroscopy. *J. Phys. Chem. C* **2025,** *129* (39), 17643-17652.
31. Lustemberg, P. G.; Plessow, P. N.; Wang, Y.; Yang, C.; Nefedov, A.; Studt, F.; Wöll, C.; Ganduglia-Pirovano, M. V., Vibrational frequencies of cerium-oxide-bound CO: A challenge for conventional DFT methods. *Phys. Rev. Lett.* **2020,** *125* (25), 256101.
32. Lustemberg, P. G.; Yang, C.; Wang, Y.; Wöll, C.; Ganduglia-Pirovano, M. V., Vibrational frequencies of CO bound to all three low-index cerium oxide surfaces: A consistent theoretical description of vacancy-induced changes using density functional theory. *J. Chem. Phys.* **2023,** *159* (3).
33. Dolling, D. S.; Chen, J. C.; Schober, J. C.; Creutzburg, M.; Jeromin, A.; Vonk, V.; Sharapa, D. I.; Keller, T. F.; Plessow, P. N.; Noei, H.; Stierle, A., Probing Active Sites on Pd/Pt Alloy Nanoparticles by CO Adsorption. *Acs Nano* **2024,** *18* (45), 31098-31108.
34. Wang, J.; Sauter, E.; Nefedov, A.; Heißler, S.; Maurer, F.; Casapu, M.; Grunwaldt, J.-D.; Wang, Y.; Wöll, C., Dynamic structural evolution of ceria-supported Pt particles: a thorough spectroscopic study. *J. Phys. Chem. C* **2022,** *126* (21), 9051-9058.
35. Gashnikova, D.; Maurer, F.; Sauter, E.; Bernart, S.; Jelic, J.; Dolcet, P.; Maliakkal, C. B.; Wang, Y. M.; Wöll, C.; Studt, F.; Kübel, C.; Casapu, M.; Grunwaldt, J. D., Highly Active Oxidation Catalysts through Confining Pd Clusters on CeO2 Nano-Islands. *Angewandte Chemie-International Edition* **2024,** *63* (35).
36. Zhou, D.; Wang, J.; Jian, M.; Li, Y.; Jiang, Z.; Liu, S.; Zhou, Y.; Wei, J.; Wöll, C.; Li, W.-X., Fine-tuned coordination environment of Pt-Fe-Pt active site for selective heterogeneous hydrogenation of crotonaldehyde. *Chem* **2025,** *11* (5), 102380.

37. Wang, B.; Yu, Z. R.; Chen, S.; Da Roit, N.; Schild, D.; Zimmermann, M.; Wang, Y. M.; Behrens, S., Single-Step Synthesis of Dimethyl Ether from Syngas over Nanoparticle-Derived Bifunctional Pd/CeO2/Al2O3 Catalysts. *Angewandte Chemie-International Edition* **2025,** *64* (16).
38. Kresse, G.; Furthmuller, J., Efficiency of ab-initio total energy calculations for metals and semiconductors using a plane-wave basis set. *Computational Materials Science* **1996,** *6* (1), 15-50.
39. Kresse, G.; Hafner, J., ABINITIO MOLECULAR-DYNAMICS FOR LIQUID-METALS. *Physical Review B* **1993,** *47* (1), 558-561.
40. Wellendorff, J.; Lundgaard, K. T.; Mogelhoj, A.; Petzold, V.; Landis, D. D.; Norskov, J. K.; Bligaard, T.; Jacobsen, K. W., Density functionals for surface science: Exchange-correlation model development with Bayesian error estimation. *Physical Review B* **2012,** *85* (23).
41. Kresse, G.; Joubert, D., From ultrasoft pseudopotentials to the projector augmented-wave method. *Physical Review B* **1999,** *59* (3), 1758-1775.
42. Dudarev, S. L.; Botton, G. A.; Savrasov, S. Y.; Humphreys, C. J.; Sutton, A. P., Electron-energy-loss spectra and the structural stability of nickel oxide: An LSDA+U study. *Physical Review B* **1998,** *57* (3), 1505-1509.
43. Maurer, F.; Beck, A.; Jelic, J.; Wang, W.; Mangold, S.; Stehle, M.; Wang, D.; Dolcet, P.; Gänzler, A. M.; Kübel, C.; Studt, F.; Casapu, M.; Grunwaldt, J. D., Surface Noble Metal Concentration on Ceria as a Key Descriptor for Efficient Catalytic CO Oxidation. *Acs Catalysis* **2022,** *12* (4), 2473-2486.
44. Monkhorst, H. J.; Pack, J. D., SPECIAL POINTS FOR BRILLOUIN-ZONE INTEGRATIONS. Physical Review B 1976, 13 (12), 5188-5192.
45. Meunier, F. C., Relevance of IR Spectroscopy of Adsorbed CO for the Characterization of Heterogeneous Catalysts Containing Isolated Atoms. *J. Phys. Chem. C* **2021,** *125* (40), 21810-21823.
46. Barama, N. E.; Wang, C. L.; Sombut, P.; Rath, D.; Lagin, A.; Ormos, M.; Puntscher, L.; Lewis, F. J.; Jakub, Z.; Kraushofer, F.; Eder, M.; Meier, M.; Schmid, M.; Diebold, U.; Franchini, C.; Matvija, P.; Pavelec, J.; Parkinson, G. S., CO on a Rh/Fe3O4 single-atom catalyst: high-resolution infrared spectroscopy and near-ambient-pressure scanning tunnelling microscopy. *Faraday Discussions* **2026**.